Since January 2020 Elsevier has created a COVID-19 resource centre with free information in English and Mandarin on the novel coronavirus COVID-19. The COVID-19 resource centre is hosted on Elsevier Connect, the company's public news and information website.

Clinical Immunology 247 (2023) 109240

Contents lists available at ScienceDirect

Clinical Immunology

journal homepage: www.elsevier.com/locate/yclim

Down-regulation of KLF2 in lung fibroblasts is linked with COVID-19 immunofibrosis and restored by combined inhibition of NETs, JAK-1/2 and IL-6 signaling

Akrivi Chrysanthopoulou [a,1], Christina Antoniadou [b,1], Anastasia-Maria Natsi [a,1], Efstratios Gavriilidis [b], Vasileios Papadopoulos [b], Evangelia Xingi [c], Stylianos Didaskalou [d], Dimitrios Mikroulis [e], Victoria Tsironidou [a], Konstantinos Kambas [f], Maria Koffa [d], Panagiotis Skendros [a,b,**,2], Konstantinos Ritis [a,b,*,2]

[a] Laboratory of Molecular Hematology, Department of Medicine, Democritus University of Thrace, Alexandroupolis, Greece
[b] First Department of Internal Medicine, University Hospital of Alexandroupolis, Democritus University of Thrace, Alexandroupolis, Greece
[c] Light Microscopy Unit, Hellenic Pasteur Institute, Athens, Greece
[d] Laboratory of Cell Biology, Proteomics and Cell Cycle, Department of Molecular Biology and Genetics, Democritus University of Thrace, Alexandroupolis, Greece
[e] Department of Cardiovascular Surgery, University Hospital of Alexandroupolis, Democritus University of Thrace, Alexandroupolis, Greece
[f] Laboratory of Molecular Genetics, Department of Immunology, Hellenic Pasteur Institute, Athens, Greece

ARTICLE INFO

Keywords:
COVID-19
Immunofibrosis
KLF2
DNase I
Tocilizumab
Baricitinib

ABSTRACT

Kruppel-like factor 2 (KLF2) has been linked with fibrosis and neutrophil-associated thromboinflammation; however, its role in COVID-19 remains elusive. We investigated the effect of disease microenvironment on the fibrotic potential of human lung fibroblasts (LFs) and its association with KLF2 expression. LFs stimulated with plasma from severe COVID-19 patients down-regulated KLF2 expression at mRNA/protein and functional level acquiring a pre-fibrotic phenotype, as indicated by increased CCN2/collagen levels. Pre-incubation with the COMBI-treatment-agents (DNase I and JAKs/IL-6 inhibitors baricitinib/tocilizumab) restored KLF2 levels of LFs to normal abolishing their fibrotic activity. LFs stimulated with plasma from COMBI-treated patients at day-7 expressed lower CCN2 and higher KLF2 levels, compared to plasma prior-to-treatment, an effect not observed in standard-of-care treatment. In line with this, COMBI-treated patients had better outcome than standard-of-care group. These data link fibroblast KLF2 with NETosis and JAK/IL-6 signaling, suggesting the potential of combined therapeutic strategies in immunofibrotic diseases, such as COVID-19.

1. Introduction

Pulmonary fibrosis is one of the major complications of COVID-19, as its degree can affect the outcome of the patients. In addition, fibrosis is a frequently reported post-infectious lung sequela, affecting a substantial number of COVID-19 survivors [1,2]. Recent studies indicate that fibrotic lung lesions may be related to the severity and duration of COVID-19 and develop during the late phases in the course of the disease, usually after the third week from the onset of symptoms [3–7]. Moreover, fibrosis in COVID-19 involves structural remodeling of the lung, in which the mesenchymal cells of lung interstitium and primarily the fibroblasts play the pivotal role [4,8–12]. Innate immune cells infiltration, release of pro-inflammatory cytokines, complement activation and endothelial injury are key drivers for the initiation and maintenance of excessive inflammation within the lung microenvironment [3,8–14]. All these pathways converge towards the proliferation

* Correspondence to: Konstantinos Ritis, Laboratory of Molecular Hematology, Department of Medicine, Democritus University of Thrace, Alexandroupolis 68100, Greece.
** Correspondence to: Panagiotis Skendros, First Department of Internal Medicine, University Hospital of Alexandroupolis, Democritus University of Thrace, Alexandroupolis 68100, Greece.
E-mail addresses: pskendro@med.duth.gr (P. Skendros), kritis@med.duth.gr (K. Ritis).
[1] Contributed equally to this work.
[2] Shared supervision of the study.

https://doi.org/10.1016/j.clim.2023.109240
Received 20 November 2022; Received in revised form 17 January 2023; Accepted 18 January 2023
Available online 21 January 2023

and activation of lung fibroblasts (LFs), which produce matricellular proteins and collagen, leading to fibrotic remodeling [8,12,15]. Cellular communication network factor 2 (CCN2) expression in activated fibroblasts is critically associated with tissue fibrosis and has been widely used as a marker of the fibrotic process in several diseases [15,16]. Apart from the production of extracellular matrix proteins, LFs have multiple concomitant biological roles. LFs do not constitute passive bystanders to the inflammatory stimuli; they can be differentiated into functionally dynamic cells producing bioactive molecules, such as pro-inflammatory cytokines, tissue factor (TF) and growth factors that maintain and feedback the thromboinflammatory state [17–19].

Krüppel-like factor 2 (KLF2) is a transcription factor involved in multiple cellular regulatory processes in different tissues [20–22]. Its protective role is well established in endothelial cells, where it promotes vascular homeostasis, quiescence, and integrity [20,23,24]. In experimental models of ARDS, as well as in lung autopsies of COVID-19 patients, downregulation of endothelial KLF2 has been associated with severe endothelial dysfunction [24–26]. KLF2 has also been described in animal models of fibrotic diseases such as bleomycin-induced pulmonary fibrosis and cirrhosis [27,28] indicating that its downregulation is associated with disease progression, whilst overexpression exerts antifibrotic effects. However, the role of KLF2 in lung fibroblast in the context of COVID-19-related inflammation has not been elucidated yet.

Recently, our group suggested the important role of LFs in the context of COVID-19 immunothrombosis by linking disease inflammatory environment with the expression and activity of TF in these cells. Moreover, combined *in vitro* administration of pharmaceutical agents against neutrophil extracellular traps (NETs), JAK-1/2 and IL-6 significantly reduced functional TF expression in LFs, providing a possible explanation for the observed beneficial effect of these drugs in a cohort of severe COVID-19 patients [17].

This study aims to investigate the presence of a mechanistic link between COVID-19-mediated immunofibrosis and KLF2 expression in human lung fibroblasts. Moreover, in severely affected patients, disease outcome after administration of a combined rescue treatment targeting NETs, JAK-1/2 and IL-6 signaling is studied, and correlated with the fibrotic potential of human lung fibroblasts and their alterations in KLF2 expression.

2. Material and methods

2.1. Patients

We recruited 94 non-intensive care unit (ICU) patients (Table 1) with COVID-19-associated severe respiratory failure (SRF), as defined by $PaO_2/FiO_2 < 100$ mmHg. Patients were admitted in wards from April 1, 2021 to December 31, 2021 in the First Department of Internal Medicine at University Hospital of Alexandroupolis, a tertiary care hospital for COVID-19 in Greece (https://clinicaltrials.gov/ct2/show/NCT05279391). The inclusion criteria were as follows: 1) adult patients ≥18 years old, 2) positive polymerase-chain-reaction (PCR) test or rapid-antigen test for SARS-CoV-2 in nasopharyngeal swab, 3) pulmonary infiltrates suggestive of COVID-19, 4) progression to SRF, 5) written informed consent from the patients or their legal representatives for the COMBI compassionate therapeutic protocol.

Patients meeting the following criteria, were excluded: 1) need for intubation/IMV during the first 24 h after the initiation of treatment, 2) multi-organ failure, 3) systemic co-infection, 4) SRF due to cardiac failure or fluid overload, 5) glomerular filtration rate (GFR) <30 ml/min/1.73 m^2, 6) any stage IV solid tumor or immunosuppression due to hematological disorders, 7) any immunosuppressive therapy and/or chemotherapy during the last 30 days, 8) low patient's functional performance status as defined by a Palliative Performance Scale (PPS) score ≤ 30% [29], 9) pregnancy. None of the patients had been infected by the Omicron variant of SARS-CoV-2.

Two groups were analyzed and compared: the Standard-of-Care (SOC) group ($n = 21$), consisting of patients who received dexamethasone, low molecular weight heparin (LMWH) and supportive care, and the COMBI group ($n = 73$), consisting of patients who received, on top of SOC, the following combination regimen: a) tocilizumab, an anti-IL-6 receptor antagonist, in a single intravenous dose of 8 mg/kg actual body weight up to 800 mg, b) baricitinib, a selective JAK-1/JAK-2 inhibitor, 4 mg *per os* once daily, for up to 14 days (2 mg once daily, if GFR was 30–60 ml/min/1.73 m2), and c) nebulized dornase alfa, a recombinant human DNase I (inhaled DNase), 2500 U/twice daily for up to 14 days. Inhaled DNase was administered simultaneously with inhaled budesonide (800 μg/twice daily) and bronchodilators (salbutamol or/and ipratropium at standard doses).

Table 1
Baseline demographic and clinical characteristics of the patients studied ($n = 94$).

Parameter	COMBI (n = 73)	Non-COMBI ($n = 21$)	*P*
Age (years)			
Mean ± SD	58.6 ± 10.6	62.8 ± 9.1	0.082
Sex			
Male (%)	45 (61.6)	12 (57.1)	0.710
Female (%)	28 (38.4)	9 (42.9)	
Body Mass Index (BMI)			
Mean ± SD	30.4 ± 4.1	30.8 ± 4.8	0.775
Vaccination status*			
Vaccinated (%)	12 (16.4)	4 (19.0)	0.779
Number of comorbidities			
Mean ± SD	1.5 ± 1.2	1.7 ± 1.1	0.495
Comorbidities			
Obesity (BMI ≥ 30) (%)	33 (45.2)	9 (42.9)	0.849
Essential hypertension (%)	40 (54.8)	14 (66.7)	0.332
Diabetes mellitus (%)	14 (19.1)	8 (38.1)	0.071
Coronary artery disease (%)	7 (9.6)	3 (14.2)	0.539
Heart failure (%)	2 (2.7)	0 (0)	1.000
Atrial fibrillation (%)	3 (4.1)	1 (4.8)	1.000
Chronic obstructive pulmonary disease/Asthma (%)	6 (8.2)	1 (4.8)	1.000
Chronic kidney disease# (%)	2 (2.7)	0 (0)	1.000
Disease day at admission			
Mean ± SD	9.4 ± 2.6	8.6 ± 2.0	0.191

* Considering patients who were fully vaccinated against SARS COV-2 based on the current vaccination recommendations, for each time period of study.
\# All patients had GFR > 30 ml/min/1.73m^2.

The study protocol design was approved by the Local Scientific and Ethics Committees of the University Hospital of Alexandroupolis, Greece (Ref. No. 87/08-04-2020). All subjects provided written informed consent in accordance with the principles expressed in the Declaration of Helsinki. Patients' records were anonymized and deidentified prior to analysis, to ensure confidentiality and anonymity.

2.2. Plasma collection

To isolate plasma, venous blood from either healthy individuals or COVID-19 patients was collected in BD vacutainer® EDTA tubes (Becton Dickinson and Company) and then centrifuged at 500 ×*g* for 15 min. COVID-19 plasma was collected from patients before treatment administration and at day 7 of COMBI (COMBI day 7) or SOC (SOC day 7) treatment. To isolate platelet-rich plasma (PRP), venous blood either from healthy subjects or treatment-naive COVID-19 patients was collected in BD Vacutainer® citrate tubes (Becton Dickinson and Company) and then centrifuged at 150 ×*g* for 10 min. Then, samples were stored at −80 °C.

2.3. Neutrophil isolation

Peripheral heparinized blood was collected from healthy individuals. Peripheral neutrophils were isolated by Histopaque double-gradient density centrifugation (11,191 and 10,771, Sigma-Aldrich) at 700 ×*g*

for 30 min [30]. Then, cells were washed with phosphate-buffered saline (PBS-1×) and centrifuged at 200 ×*g* for 12 min. Cell purity was estimated ≥98%.

2.4. Stimulation and inhibition studies in isolated human neutrophils

Neutrophils isolated from healthy donors were resuspended in Roswell Park Memorial Institute (RPMI) medium (Thermo Fisher Scientific) supplemented with 2% FBS. Then, they were stimulated for 3 h at 37 °C and 5% CO_2 with 3% PRP, derived from COVID-19 patients, to generate NETs. The concentrations and time points used to test neutrophil function were optimized before the experiments. All substances used were endotoxin free, as determined by a Limulus amebocyte assay (E8029, Sigma-Aldrich).

2.5. NET generation and collection

A total of 1.5 × 10^6 neutrophils were cultured in RPMI culture medium for 3.5 h in the presence of PRP, as described in the above section. Unstimulated neutrophils served as control (control NETs). Afterwards, the medium was removed, and cells were washed twice with prewarmed RPMI medium. NET structures were collected in the supernatant phase, upon vigorous agitation of the culture plate and centrifugation at 20 ×*g* for 5 min [31,32]. They were kept undigested at -20 °C till analyzed. The quantification of NETs in supernatants was assessed by MPO/DNA complex ELISA (Cell Death Detection ELISA Kit, Merck), as previously described [33].

2.6. Human lung fibroblasts (LFs) isolation, culture and characterization

Primary human lung fibroblasts (LFs) were isolated from healthy lung tissue obtained during open lung biopsy from three donors at the University Hospital of Alexandroupolis, Greece, as described previously [34,35]. LFs were cultured in Dulbecco's modified Eagle's medium (DMEM; Thermo Fisher Scientific), supplemented with 10% fetal bovine serum (FBS; Thermo Fisher Scientific) and 100 U/ml antibiotic/antimycotic solution (Thermo Fisher Scientific) at 37 °C and 5% CO_2. LFs in passages 2–4 were used. Before each experiment, cells were stained using mouse monoclonal antibodies against alpha-smooth muscle actin (α-SMA), vimentin, and desmin (Thermo Fisher Scientific) to verify their phenotype [34].

2.7. Stimulation and inhibition studies in human lung fibroblasts

LFs were stimulated with EDTA plasma derived from either healthy donors or COVID-19 patients, as described above, at a final concentration of 2% in DMEM. Cells were also incubated with *in-vitro* generated NET structures (*i.e.* control neutrophils stimulated with COVID-19 PRP) at a final concentration of 20% in DMEM.

Cell culture supernatant released from LFs upon stimulation with 2% EDTA plasma derived from treatment-naïve COVID-19 patients (4 h) was characterized by increased TF activity [17]. Therefore, supernatant was collected and subsequently used to examine autocrine effect in our set of experiments. Supernatant collected from LFs upon incubation with 2% EDTA plasma from healthy individuals was used as control.

To block IL-6 signaling, LFs were pre-treated (60 min) with tocilizumab – a humanized monoclonal antibody against interleukin-6 receptor (1 μg/ml; Actemra, Hoffmann-La Roche). To inhibit Janus kinase signaling (JAK-1 and JAK-2), cells were pre-treated (60 min) with baricitinib (2.5 nM; Olumiant, Lilly). To dismantle NETs, EDTA plasma or *in-vitro* generated NETs were pre-incubated (60 min) with DNase I (1 U/ml; EN0525, Thermo Fisher Scientific). To inhibit thrombin, EDTA plasma was pre-treated (60 min) with dabigatran (Boehringer Ingelheim International GmbH). To hinder protease-activated receptor-1 (PAR-1) signaling, LFs were pre-treated (60 min) with FLLRN peptide (250 uM; Anaspec). The *in vitro* combined inhibition (COMBI) consists of tocilizumab, baricitinib and DNase I mixture in the abovementioned concentrations.

For mRNA expression studies, LFs were stimulated for 3 h. To trigger the expression of KLF2, LFs were further stimulated with Tannic acid (2 nM; Sigma-Aldrich), a polyphenolic compound, acting as a potent inducer of KLF2 [36]. The concentrations and time points used to investigate LFs function were optimized before the experiments. All substances used were endotoxin free, as determined by a Limulus amebocyte assay.

2.8. RNA isolation, cDNA synthesis and qPCR

RNA isolation and cDNA synthesis were conducted in LFs, as previously described [34,35]. Real-time qPCR for Krüppel-like Factor 2 (KLF2) or/and connective tissue growth factor (CCN2) was performed. To normalize the expression of the above-mentioned genes, glyceraldehyde 3-phosphate dehydrogenase (GAPDH) was used as an internal control gene. Details regarding the primers and conditions of qPCR are given in Supplementary Table 1. The data were analyzed using the $2^{-\Delta\Delta Ct}$ mathematical model [37].

2.9. In-cell ELISA (cytoblot)

To study the intracellular protein expression of CCN2 or KLF2, LFs were cultured in 96-well high-binding microplates (Thermo Fisher Scientific) in the presence of distinct stimuli for 4 h. Cells were fixed with 4% paraformaldehyde (30 min; Sigma-Aldrich), permed using 1× permeabilization buffer (30 min; Abcam) and blocked using 2× blocking solution (2 h; Abcam). Upon washes with PBS-1×, cells were incubated overnight with either goat anti-CCN2 monoclonal antibody (2 μg/ml; Santa Cruz Biotechnology Inc) or mouse anti-KLF2 monoclonal antibody (6 μg/ml; Thermo Fisher Scientific). Next, a horseradish peroxidase–conjugated rabbit anti–goat IgG (1:2000 dilution, R&D Systems) or rabbit anti–mouse IgG (1:2000 dilution, R&D Systems), respectively, was added in cells for 1 h. Cells were thoroughly washed with PBS-1× and then TMB substrate was added. Microplates were measured at 650 nm. The corrections were performed by subtracting the signal of the wells incubated in the absence of primary antibody [17,38,39].

2.10. Immunofluorescence staining

LFs were cultured in chambered slides or 24-well cell culture plates (Ibidi) and they were treated with various stimuli for 4 h. Cells were fixed with 4% paraformaldehyde (Sigma-Aldrich), and non-specific binding sites were blocked with 6% normal goat serum (Thermo Fisher Scientific) in PBS 1× [17,38]. Upon blocking, cells were stained using a goat anti-CCN2 monoclonal antibody (1:100 dilution; Santa Cruz Biotechnology Inc) or a mouse anti-KLF2 monoclonal antibody (6 μg/ml concentration; Thermo Fisher Scientific) or a rabbit anti-vimentin monoclonal antibody (1:300 dilution; Abcam). After thorough washes in PBS-1×, a polyclonal donkey anti-goat IgG AlexaFluor 488 antibody (Thermo Fisher Scientific) or a polyclonal rabbit anti-mouse IgG AlexaFluor 488 antibody (Thermo Fisher Scientific) or a polyclonal goat anti-rabbit IgG AlexaFluor 647 antibody (Thermo Fisher Scientific) was utilized as the secondary antibody. A mounting medium with DAPI (counterstaining, Ibidi) was used in the final step. Visualization was performed on an Andor Revolution Spinning Disk Confocal system (Yokogawa CSU-X1) build around an Olympus IX81 microscope mounted with a 40× (0.95NA) or a 4× (0.13NA) air lenses and a digital camera (Andor Ixon Ultra 897) (Bioimaging-DUTH facility). System components were controlled by Andor IQ3.6 software.

Quantification was performed using Imaris v 9.3.1 image analysis software. In particular, a surface was created based on the fluorescence signal and mean intensity of the KLF2 staining was measured in images of untreated and treated samples.

2.11. Collagen measurement

The soluble collagen types (I—V) were determined using a Sircol Collagen Assay Kit. Briefly, LFs were cultured in 6-well plates (Thermo Fisher Scientific), treated with various agents and the culture supernatant was collected after 24 h. Cell debris was removed by centrifugation and the resulting supernatant was incubated overnight with isolation and concentration reagent, provided with the kit, at 4 °C. Afterwards, the assay was conducted according to the manufacturer protocol (Biocolor) as previously described [35].

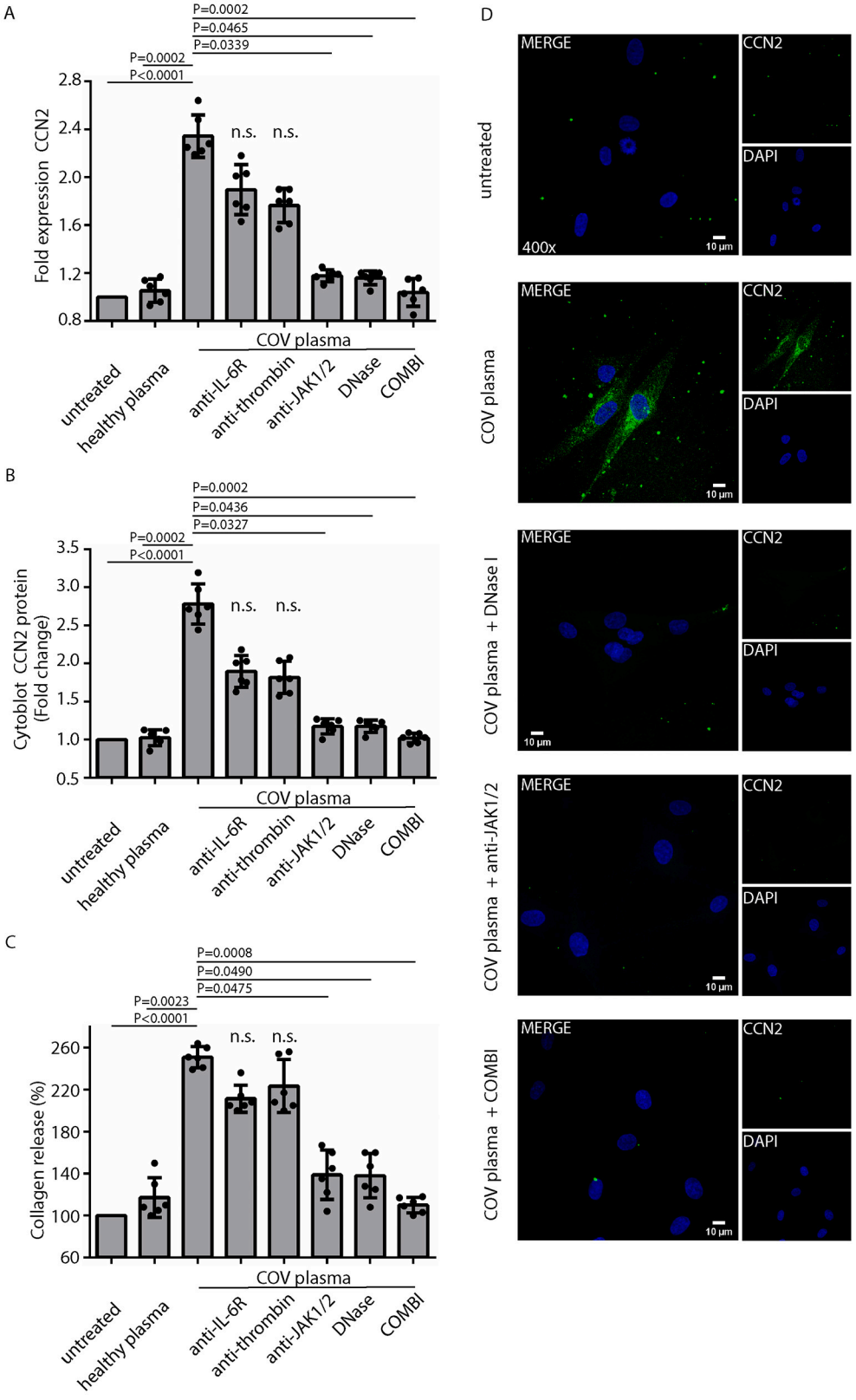

Fig. 1. Inhibition studies on fibrotic potential of human lung fibroblasts treated with COVID-19 plasma. Lung fibroblasts (LFs) were stimulated with COVID-19-derived plasma and inhibited with an anti-IL-6 receptor monoclonal antibody (tocilizumab), or a selective thrombin inhibitor (dabigatran), or a selective JAK1/JAK2 inhibitor (baricitinib), or DNase I or a combination of DNase I plus baricitinib and tocilizumab (COMBI treatment). Assessment of CCN2 expression by (A) qPCR, (B) In-Cell ELISA (Cytoblot). (C) Collagen assay of LFs supernatants. The effect of therapeutic agents was compared to conditions of LFs cultures treated only with COVID-19 plasma, $n = 6$, bars represent mean ± SD, statistical significance was set at $p < 0.05$ (n.s.: not significant), *Kruskal–Wallis* test. (D) CCN2 immunostaining in confocal fluorescence microscopy. One representative example out of three independent experiments is shown. Scale bar = 10 µm, Magnification = 400×.

2.12. TF activity assay

After 4 h of cell stimulation, TF activity was measured in cell supernatant [38] using Tissue Factor Human Chromogenic Activity Assay Kit (ab108906, Abcam), in accordance to the manufacturer's instructions. In brief, the assay measures the ability of TF/FVIIa to activate factor X to Xa. The change in absorbance of the chromophore is directly proportional to the TF enzymatic activity. For the reliability of our results, TF activity was also evaluated directly in the plasma samples that were then used as stimuli in cell cultures. In this case, plasma samples were diluted in DMEM, at the final concentration of 2%, to resemble culture conditions. These values served as controls of the assay.

2.13. Wound healing assay

The migratory capacity of LFs was assessed by performing a wound healing-migration assay according to the manufacturer's instructions and as previously performed [35]. Briefly, LFs were seeded in a 24-well culture plate containing silicone inserts (Ibidi) till cell attachment. Then, inserts were removed to generate a 0.5-mm "cell free area". Cells were incubated with appropriate agents for 18 h and then healing process was evaluated. In particular, in the initial experiments, cells were stained with May Grünwald-Giemsa and visualized by reverse light microscope (Axiovert 25; Zeiss). In the next experiments, cells were stained with monoclonal antibodies against KLF2 and vimentin, as described above in the "Immunofluorescence Section", and visualized in a spinning disc confocal microscope (BioImaging-DUTH facility).

2.14. Statistical analysis

Comparisons among more than two groups of data, were performed using Kruskal-Wallis test, followed by Dunn's test for multiple comparisons. The strength of linear relation between KLF2 and CCN2 was measured with Pearson's correlation coefficient. Wilcoxon signed-rank test was used to compare matched samples. Comparisons between two independent groups were performed using Student's *t*-test with Welch correction (2-tailed). Chi square test was used to compare outcomes between the two treatment groups. In parallel, Chi square, Fischer's exact test and ANOVA were used to compare binary and continuous variables, as potential confounders. Kaplan-Meier curves were used to depict survival data; comparisons were performed by the Log-rank (Mantel-Cox) test. The level of statistical significance was set at 0.05. Statistical analysis and graphs were created using SPSS 26.0 and GraphPad Prism 6.0 respectively.

3. Results

3.1. Inflammatory environment of COVID-19 plasma is involved in the fibrotic potential of human lung fibroblasts

In view that COVID-19 pathogenesis is shaped by a complex interaction of soluble mediators and cellular components [10,40,41], LFs were incubated with plasma samples derived from COVID-19 patients suffering from severe respiratory failure before any immune intervention therapy. Plasma markedly induced CCN2 mRNA (Fig. 1A) and protein expression (Fig. 1B, D) along with collagen production (Fig. 1C), compared to untreated cells and control healthy plasma.

To address the role of plausible factors in plasma in the fibrotic aspects of LFs, a set of inhibition studies was performed. Since, in patients with COVID-19, elevated levels of IL-6 were observed [42,43] and triggering of immunothrombosis results in increased activity of TF/thrombin axis [13], LFs were pre-treated with a single inhibitor, namely, anti-IL-6 receptor monoclonal antibody (tocilizumab) [44] or a direct thrombin inhibitor (dabigatran) [13,45] without addition of any other inhibitory agent. Neither CCN2 expression nor collagen production was significantly reduced in COVID plasma-stimulated LFs upon these *in vitro* inhibitions (Fig. 1A-C). On the contrary, pre-treatment of LFs with a selective JAK1/JAK2 inhibitor (baricitinib) [46] or pre-incubation of plasma samples with DNase I, which dismantles the structures of NETs [10,17,47,48], significantly reduced both CCN2 expression and collagen release in plasma-stimulated LFs (Fig. 1A-D). Moreover, using NETs generated by control neutrophils treated with COVID-19 plasma (COV NETs), the fibrotic activity of LFs was enhanced, as reflected in CCN2 mRNA and protein levels (Supplementary Fig. 1A, B, D), as well as in collagen production (Supplementary Fig. 1C). This CCN2 expression and collagen production by LFs was abolished upon treatment with DNase I (Supplementary Fig. 1A-D), further supporting the potential of NET structures in the fibrotic activity of LFs.

Prompted by these findings and according to our recent clinical results [17] indicating the beneficial role of inhaled DNase I, combined with JAK and IL-6 inhibition in severe COVID-19, LFs were simultaneously inhibited against NETs, JAK and IL-6 signaling. This *in vitro* combined inhibition (COMBI treatment) resulted in a marked reduction of CCN2 expression and collagen release in culture of LFs (Fig. 1A-D).

Taken together, these *in vitro* studies indicate that NETs and JAK-STAT pathway could be considered as key partners in the ensuing COVID-19 fibrosis and COMBI treatment in COVID-19 culture conditions disrupts more efficiently the triggering of CCN2 expression and collagen release by LFs.

3.2. Tissue factor/thrombin axis induces fibrotic activity of LFs in an autocrine manner

Our recent findings have evidenced that LFs demonstrate expression of active TF under COVID-19 culture conditions [17]. Further, it is widely accepted that the coagulation system could orchestrate inflammatory and fibrotic responses in lung [13,49,50]. In line with this, we confirmed the increased activity of TF in culture supernatants collected from COVID-19 plasma-treated LFs (Fig. 2A). In parallel, we observed that LFs acquired a pre-fibrotic phenotype as indicated by the expression of CCN2 upon incubation with the culture supernatant derived from COVID-19 plasma-treated LFs (Fig. 2B-E). CCN2 mRNA and protein expression (Fig. 2B, C, E) as well as collagen production (Fig. 2D) were reduced after pre-incubation of LFs with the FLLRN peptide by hindering the thrombin signaling.

Collectively, activation of TF/thrombin axis by LFs can promote their ensuing pre-fibrotic phenotype in an autocrine manner suggesting an additional contributory mechanism which is involved in the fibrotic aspects of the disease.

3.3. COVID-19 plasma down-regulates KLF2 expression in human lung fibroblasts whereas in vitro COMBI treatment restores its levels

Since KLF2 is involved in inflammatory functions [20,21], activation of KLF2 ameliorates COVID-19-associated endothelial dysfunction [24] and is also involved in animal models of fibrosis [27,28], we sought to examine its expression in human LFs cultured in the microenvironment of COVID-19. We observed that COVID-19 plasma-treated LFs exhibit a significant down-regulation of KLF2 both in mRNA (Fig. 3A) and protein (Fig. 3B-D) levels. Next, we asked whether therapeutic agents of COMBI could restore KLF2 expression levels. Indeed, KLF2 expression was significantly up-regulated in COVID-19 plasma-stimulated LFs upon *in vitro* treatment with COMBI (Fig. 3A-D). On the other hand, the levels of KLF2 were not significantly increased upon pre-treatment of cells with a selective JAK1/JAK2 inhibitor alone (Fig. 3A-B). In the positive control cells, namely LFs incubated with tannic acid, a polyphenol KLF2 activator [36], significant upregulation of KLF2 in both mRNA and protein levels was also observed (Fig. 3A-D). In contrast to COMBI treatment, KLF2 levels were not restored in COVID-19 plasma-cultured LFs upon tannic acid stimulation (Fig. 3A-D).

Together, these data suggest that COVID-19 microenvironment suppresses KLF2 expression in LFs' cultures, while COMBI treatment

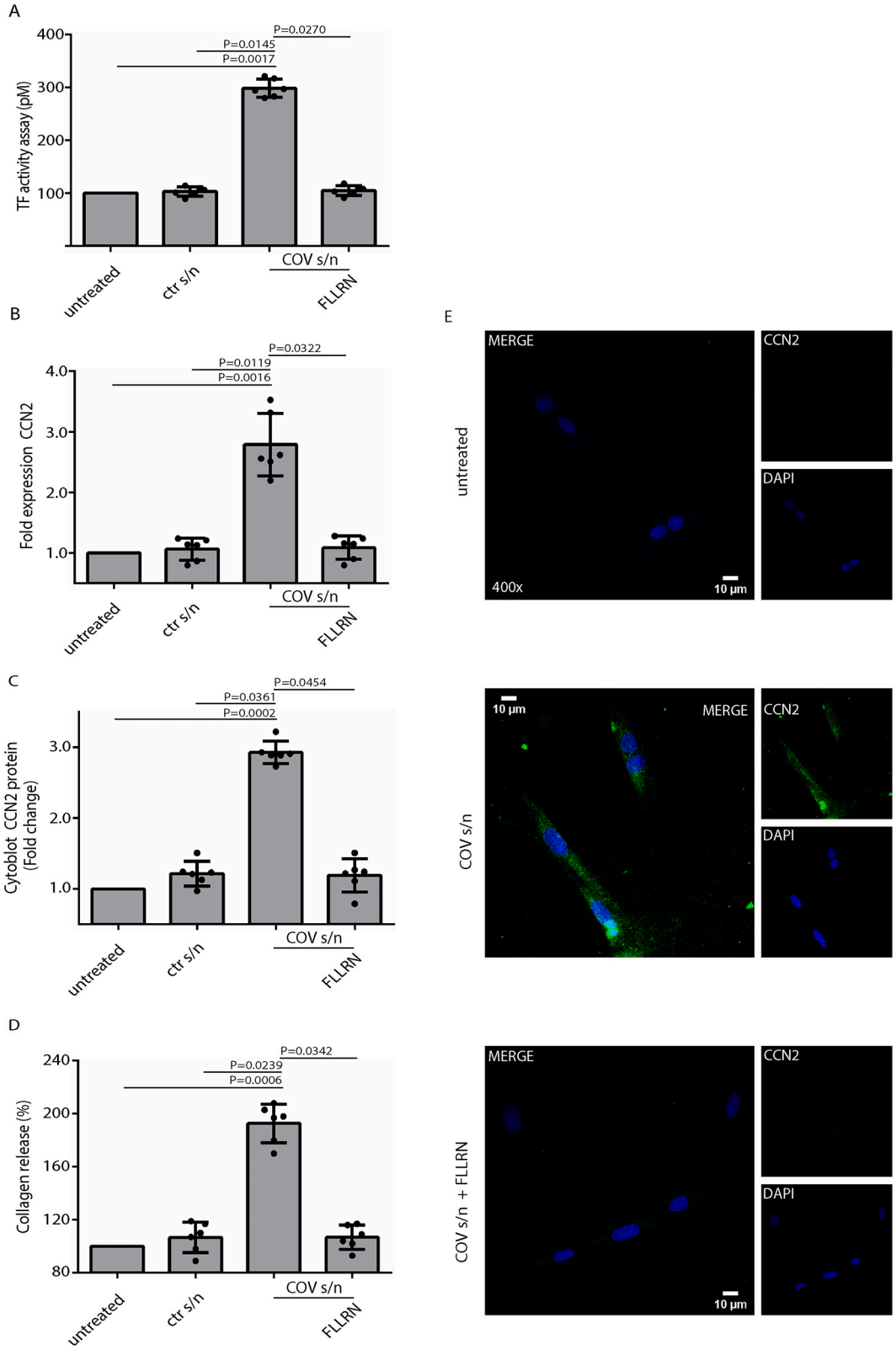

Fig. 2. Autocrine activation of human lung fibroblasts through Tissue factor/Thrombin axis. (A) TF activity was evaluated in culture supernatants collected either from COVID-19 plasma-treated lung fibroblasts (LFs) or healthy plasma-treated LFs. To hinder TF/thrombin signaling, cells were pretreated with FLLRN peptide (PAR1 receptor inhibitor). (B—D) FLLRN peptide abolished the CCN2 levels and collagen release in LFs treated with supernatants obtained from COVID-19 plasma-treated LFs. Evaluation of CCN2 expression by (B) qPCR, and (C) In-Cell ELISA (Cytoblot). (D) Collagen assay of LFs supernatants. In (B), (C) and (D) $n = 6$, bars represent mean ± SD, statistical significance was set at $p < 0.05$ (n.s.: not significant), *Kruskal–Wallis* test. (E) Immunostaining of CCN2 in confocal fluorescence microscopy (green: CCN2, blue: DAPI), one representative example out of three independent experiments is shown. Scale bar = 10 µm, Magnification = 400×. (For interpretation of the references to colour in this figure legend, the reader is referred to the web version of this article.)

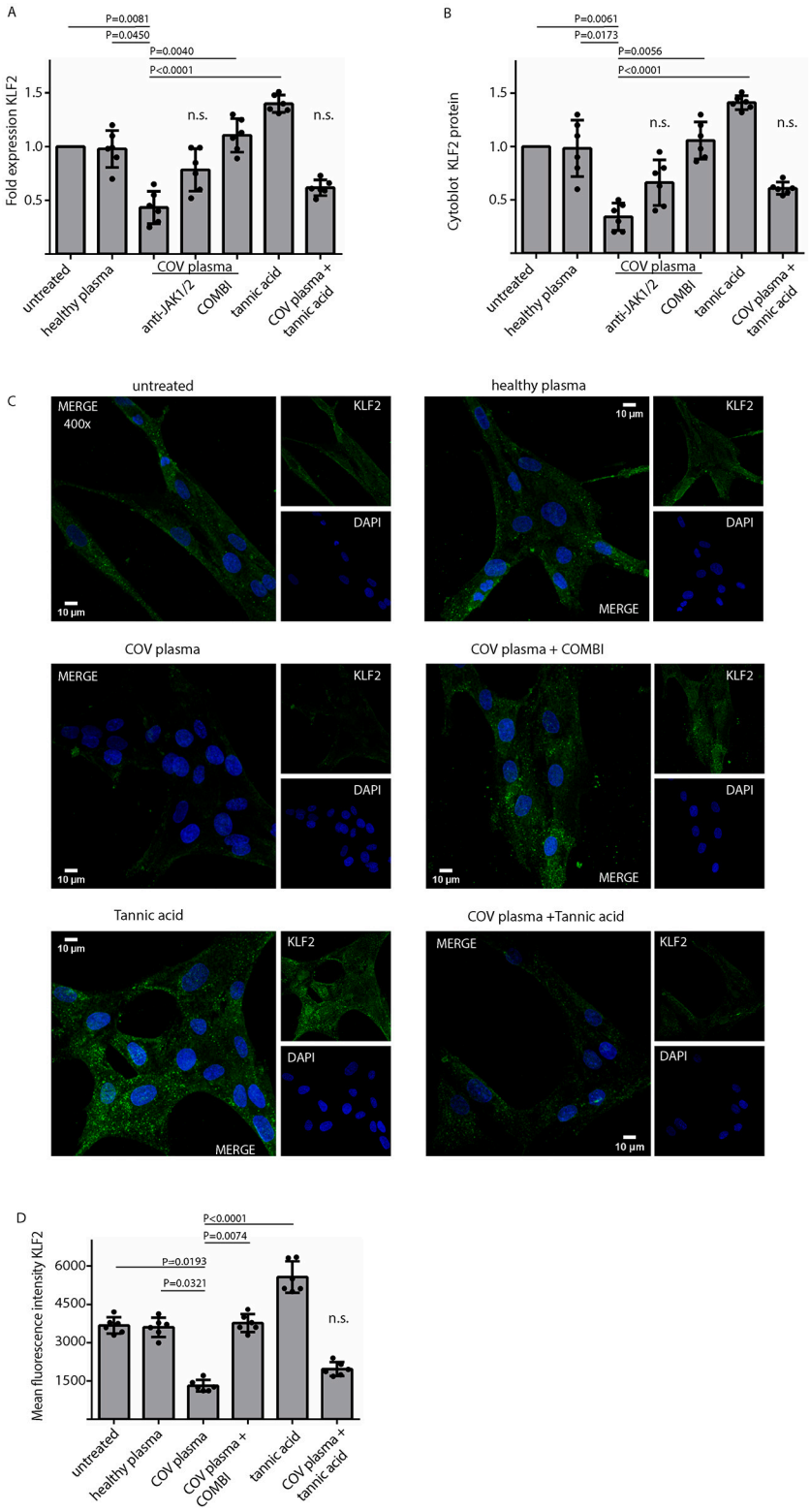

Fig. 3. Low expression of KLF2 *in* COVID-19 plasma-treated *human lung fibroblasts* is restored to normal levels after *in vitro* inhibition with COMBI agents. Lung fibroblasts (LFs) were stimulated with COVID-19-derived plasma (COV plasma). Tannic acid was used as positive control by inducing KLF2 expression. Inhibition studies were performed with a selective JAK1/JAK2 inhibitor (baricitinib) or COMBI (combination of DNase I, baricitinib and tocilizumab). *KLF2 expression was assessed by (A) qPCR and (B) In-Cell ELISA.* In (A), (B), all conditions were compared to those in LFs cultures with only COVID-19 plasma treatment, n = 6, bars represent mean ± SD, statistical significance was set at $p < 0.05$ (n.s.: not significant), *Kruskal–Wallis* test. *(C) Immunostaining of KLF2 in confocal microscopy* (green: KLF2, blue: DAPI). One representative example out of six independent experiments is shown. Scale bar = 10 μm, Magnification = 400×. In (D), the data of 6 immunofluorescence observations were further quantified and presented as mean fluorescent intensity (MFI). Bars represent mean ± SD, statistical significance was set at $p < 0.05$ (n.s.: not significant), *Kruskal–Wallis* test. (For interpretation of the references to colour in this figure legend, the reader is referred to the web version of this article.)

significantly reverses this effect.

3.4. Correlation of low expression levels of KLF2 in human lung fibroblasts with their fibrotic activity

To evaluate whether KLF2 is correlated with fibrosis in COVID-19, we treated LFs with plasma obtained from treatment-naïve COVID-19 patients suffering from respiratory failure. We found a negative correlation between mRNA levels of KLF2 and CCN2, a gene consistently associated with fibrotic remodeling (Fig. 4A).

Next, we performed a functional wound healing assay, to assess the healing process in *in vitro* conditions. Plasma from treatment-naïve patients markedly enhanced the migration rates of LFs and led to excessive healing process, whilst its impact was abrogated when cells were

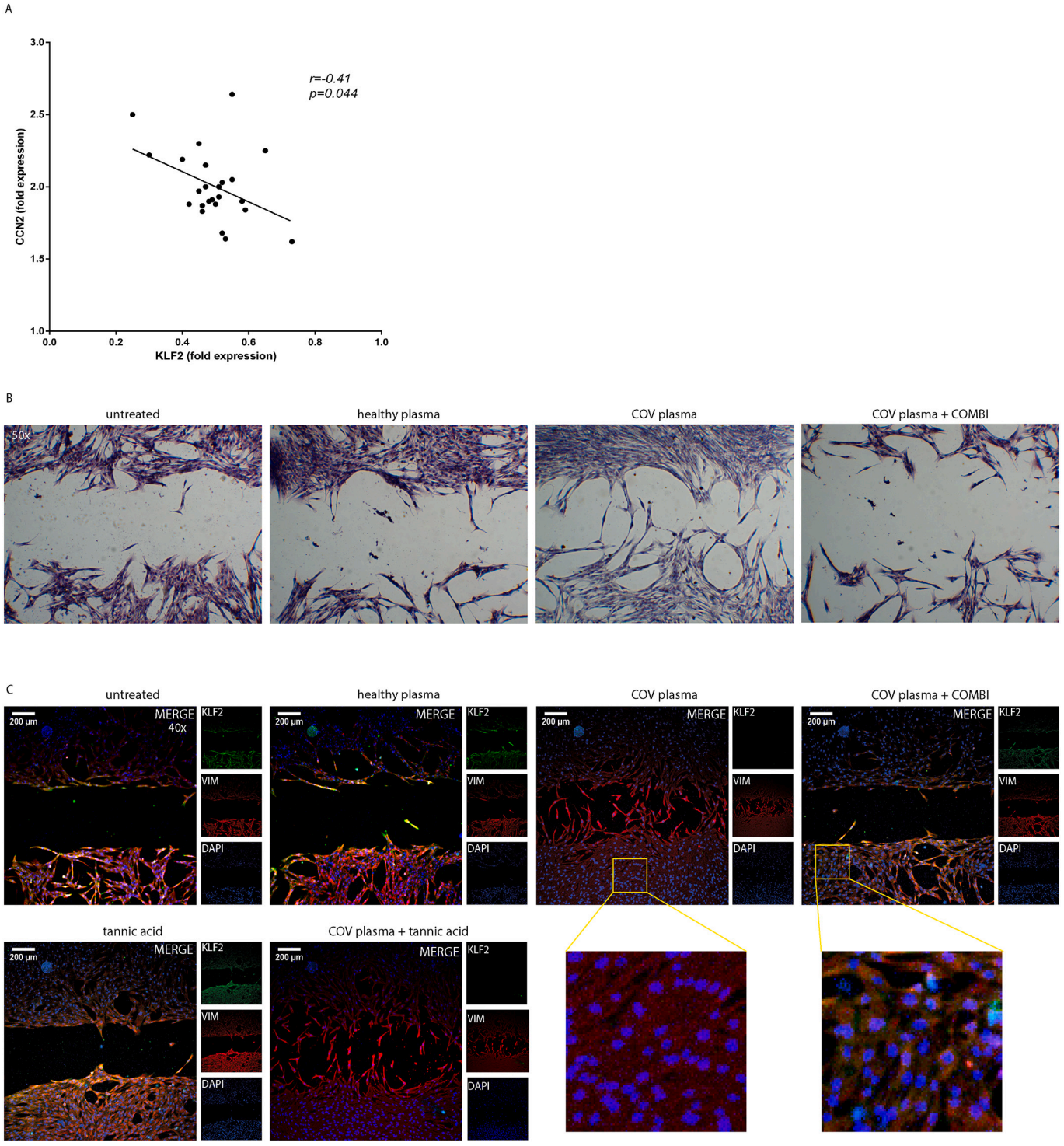

Fig. 4. The expression levels of Krüppel-like Factor 2 (KLF2) in human lung fibroblasts are correlated with their fibrotic potential. (A) Correlation between Cellular Communication Network Factor 2 (CCN2) mRNA levels and KLF2 mRNA levels in lung fibroblasts (LFs) stimulated with COVID-19-derived plasma ($n = 24$). Pearson's correlation coefficient was used. In (B), migration rate in LFs stimulated with COV plasma and inhibited with COMBI (DNase plus baricitinib and tocilizumab), assessed by inverted microscopy. In (C), immunofluorescence KLF2 expression and migration rate were assessed concurrently in LFs stimulated with either COV plasma or tannic acid as positive control (inducer of KLF2 expression). Inhibition studies with COMBI were performed and the immunostaining was assessed by confocal fluorescence microscopy [green: KLF2, red: vimentin (VIM), blue: DAPI]. In (B) and (C), untreated LFs or LFs incubated with plasma from healthy subjects were used as controls. A representative example out of three independent experiments is shown. (B) Magnification = 50× (C) Scale Bar = 200 µm, Magnification = 400×. (For interpretation of the references to colour in this figure legend, the reader is referred to the web version of this article.)

pretreated with the agents of *in vitro* COMBI protocol (Fig. 4B). Further to this assay, immunostaining of LFs revealed that the increased migratory/healing capacity of COVID-19 plasma-stimulated LFs was detected concurrently to the decrease in KLF2 protein expression (Fig. 4C). On the contrary, the *in vitro* COMBI treatment limited the migratory/healing potential of cells and KLF2 levels were increased, an effect not observed in stimulations with tannic acid (Fig. 4C).

Collectively, these findings unveil down-regulation of KLF2 in LFs as a candidate pre-fibrotic molecular event of severe of COVID-19. Moreover, COMBI immune intervention results in both restoring LFs' KLF2 levels and decreasing their migratory/healing capacity.

3.5. COMBI-treated COVID-19 patients demonstrate restoration of KLF2 low expression, as well as reduction of CCN2 levels in human lung fibroblasts resulting in favorable disease outcome

Recently, we reported initial results of an open-label observational study indicating a favorable effect of combination therapy with inhaled DNase I and inhibition of JAK and IL-6 signaling. To further validate our previous results and according to the aforementioned *in vitro* findings, we first examined whether plasma from severe COVID-19 patients receiving COMBI protocol or SOC could disparately affect the levels of KLF2 and CCN2 in LFs. Indeed, incubation with plasma isolated from COMBI group at day 7 of treatment, concurrently led to a significant percentage change in the increase of KLF2 and reduction of CCN2 in LFs, as compared to the day of admission (day 0), both in mRNA and protein levels (Fig. 5A-D). This was not true for SOC-treated patients (Fig. 5A-D).

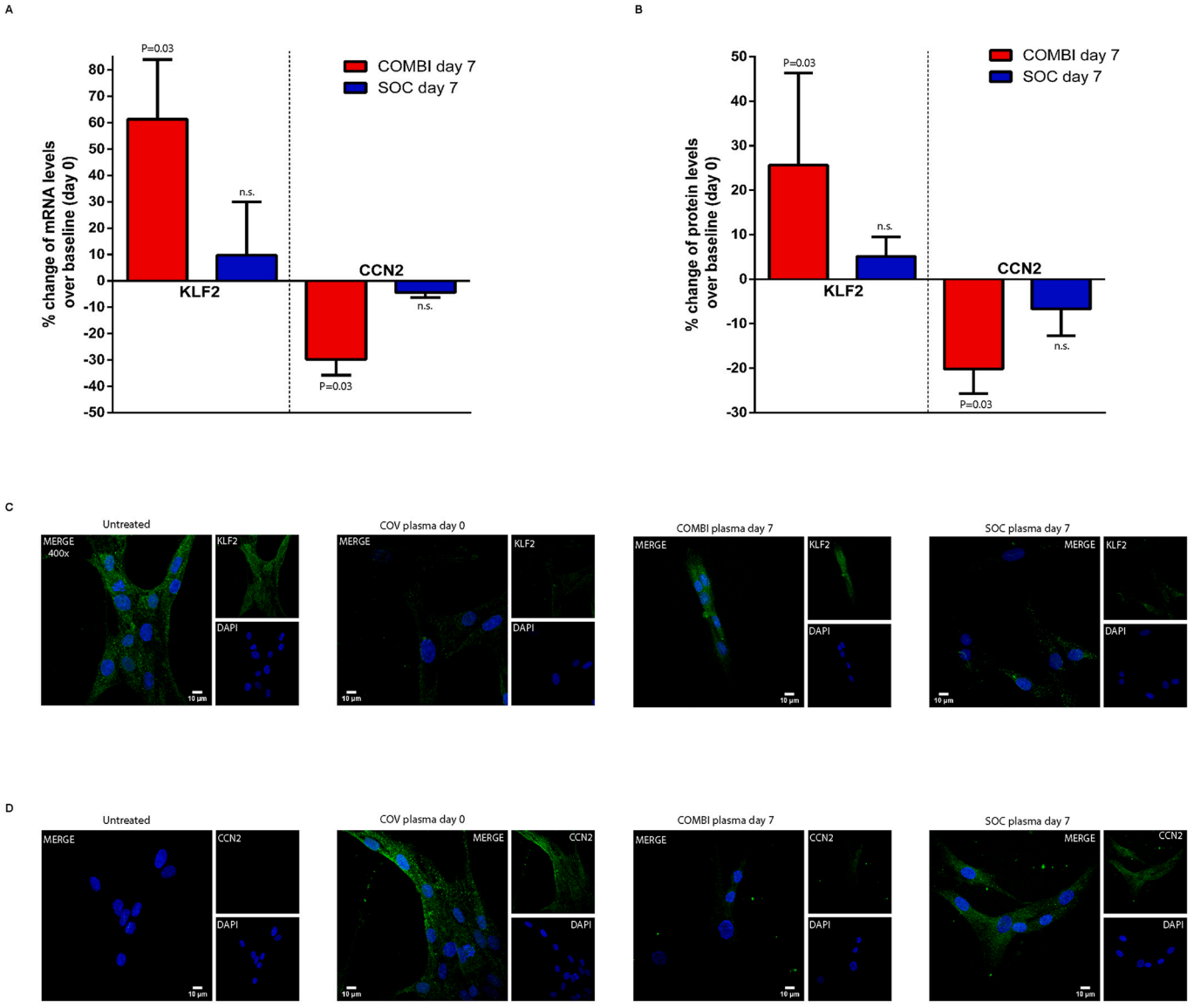

Fig. 5. Plasma, isolated from COVID-19 patients treated with COMBI protocol, increases KLF2 and suppresses CCN2 expression levels, in human lung fibroblasts. Lung fibroblasts (LFs) were stimulated with plasma from severe COVID-19 patients collected at the day of admission or plasma from the same group of patients receiving either COMBI protocol at day 7 of treatment (n = 6) or SOC protocol at day 7 of treatment (n = 6). Graphs present percentage change of mean KLF2 or CCN2 (A) mRNA levels (±SD) or (B) Cytoblot protein levels (±SD) on day 7 compared to day of admission. Paired analysis within each parameter was performed using the Wilcoxon signed-rank test. Statistical significance was set at $p < 0.05$. Confocal fluorescence microscopy showing (C) KLF2 immunostaining (green: KLF2, blue: DAPI) or (D) CCN2 immunostaining (green: CCN2, blue: DAPI) in LFs incubated with plasma from severe COVID-19 patients at the day of admission or plasma on 7th day of COMBI treatment or plasma on 7th day of SOC. One representative example out of three independent experiments is shown. Scale bar = 10 μm, Magnification = 400×. (For interpretation of the references to colour in this figure legend, the reader is referred to the web version of this article.)

Next, to translate these data, we expanded our previous clinical study analyzing in total 94 COVID-19 patients with SRF (Table 1). In the COMBI group, 11 deaths were recorded among 73 patients (15.1%). Twelve out of 73 patients were intubated (16.4%) and 11 of them did not survive. In the SOC group, 8 deaths were recorded out of 21 patients (38.1%). All these patients were intubated (38.1%) during hospitalization. Overall, COMBI protocol was associated with a significant reduction of in-hospital mortality and intubation rate compared to SOC (Fig. 6A). This therapeutic strategy was also correlated with an increase of the in-hospital survival (Fig. 6B).

Taken together, these experimental and clinical data suggest that plasma from COVID-19 patients under therapy with COMBI regimen restores the expression of KLF2 and reduces the expression of CCN2 in LFs, and that may be linked to the better clinical outcome of these patients compared to those treated with SOC.

4. Discussion

This study suggests a regulatory mechanism that links common inflammatory pathways of COVID-19 with pulmonary fibrosis, a complication substantially affecting disease outcome. We found that, upon incubation with plasma isolated from severe COVID-19 patients, LFs acquired a pre-fibrotic phenotype characterized by a high expression of CCN2 leading to excessive collagen production. Concomitantly, we observed down-regulation of KLF2 in LFs as assessed by mRNA and protein assays, as well as, by wound healing functional assay, upon incubation with COVID-19 plasma. This was well-associated with the induction of CCN2, and reversed by therapeutic agents targeting NETs, JAK-1/2 and IL-6 signaling in LFs, linking low expression of KLF2 with the fibrotic potential of LFs. Moreover, plasma obtained from patients under therapy with combination of DNase I plus JAK-1/2 and IL-6 inhibition (COMBI therapeutic protocol) was characterized by reduced capacity to induce the fibrotic activity of LFs and KLF2 down-regulation. This might further explain the observed beneficial effect of COMBI treatment in the current study and our previous findings [17].

Emerging evidence indicates that LFs are key partners of lung tissue damage in COVID-19 [4,10,41]. During disease progression, LFs accumulate and activate, repopulating the damaged alveolar wall, while simultaneously produce matricellular proteins and other bioactive molecules associated with fibrotic remodeling [8,12]. Although it is well appreciated that LFs play a pivotal role in COVID-19 progression, the pathophysiological mechanisms involved in their activation and function during the thromboinflammatory process remain elusive.

We found that human LFs treated with COVID-19 plasma, express the pre-fibrotic protein CCN2, produce collagen and demonstrate increased wound healing functional assay. In addition to the development of an uncontrolled inflammatory response, the clinical deterioration of patients with COVID-19 pneumonia, usually manifested 7–14 days after symptoms initiation, could also be attributed to the accumulation of activated fibroblasts in the affected lung tissue [4,51]. This process can be simulated and reproduced *in vitro* by observing fibrotic activation of LFs in the environment of COVID-19 plasma.

Next, we prompted to investigate candidate inhibitors against induction of CCN2 in LFs. Previously, we and others demonstrated the pre-fibrotic role of neutrophils/NETs by promoting myofibroblast differentiation and activation in several disease models [34,52–56]. In addition, several studies indicated that TF/thrombin and JAK/STAT/cytokines pathways are involved in fibroblast activation and the immunofibrotic process constituting candidate therapeutic targets [35,39,57–62]. Recently, results of our group highlighted the importance of inhibiting multiple immune-mediated pathways, to improve survival in severe COVID-19. In line with these, we explored the involvement of NETs, and JAK/STAT, IL-6, as well as TF/thrombin signaling in the observed COVID-19 plasma-mediated fibrotic activity of LFs. DNase I by dismantling NETs and JAK-1/2 blocking, used separately as single inhibitors, significantly reduced the levels of CCN2 in LFs *in vitro*. We also performed *in vitro* inhibition studies, combining the agents of COMBI therapeutic protocol (DNase I, combined with selective JAK-1/2 inhibitor baricitinib and IL-6R inhibitor tocilizumab) [17]. COMBI inhibition abolished the fibrotic activity of LFs, whereas this was not noticed when single pathway targeted therapies were used in COVID-19 plasma, such as against IL-6 or thrombin. Multiple studies indicate that immunothrombosis and induction of TF/thrombin axis are involved in COVID-19 pathology [13,17,50]. In the present study, we observed an induction of LFs fibrotic potential by TF/Thrombin axis, through an autocrine mechanism; however, thrombin inhibition alone did not significantly reduce the levels of CCN2 in COVID-19 plasma-treated LFs. We suggest that the experimental settings used in this study to prove the autocrine manner of LFs activity, constitute a “clear model”, without exogenous factors in the cultured cells. On the other hand, the single inhibition of

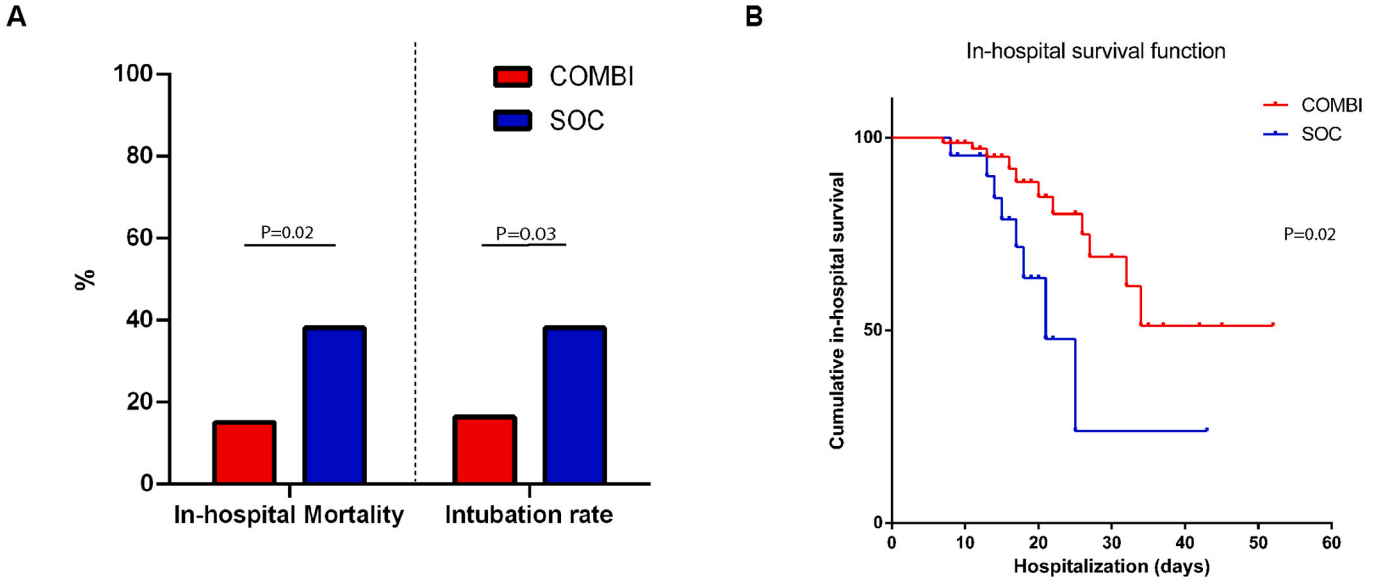

Fig. 6. Severe COVID-19 patients treated with COMBI protocol have favorable outcome. (A) COMBI treatment ($n = 73$) reduces mortality and intubation rate compared to SOC ($n = 21$). Chi square test was used. (B) COMBI increases in-hospital survival. Kaplan-Meier curves were used to visualize survival data; comparisons between groups were performed using the Log-rank test.

thrombin signaling in the COVID-19 plasma culture conditions was not sufficient to abolish the CCN2 levels in LFs, since additional pathways could be implicated. The observed abolishment of LFs' immunofibrotic activity by combined COMBI treatment suggests that multiple interconnected pathways are involved in the immunothrombotic milieu and immunofibrosis.

In the same context, we investigated the role of KLF2 in COVID-19 immunofibrosis, since this factor is widely involved in inflammatory responses [20–22], as well as in endothelial dysfunction of COVID-19 [24]. However, little is known about its effect on fibroblasts. A recent study evidenced a possible link between KLF2 and neutrophil-driven thromboinflammation [63]. Moreover, studies in animal models of bleomycin-induced pulmonary fibrosis or cirrhosis indicated the importance of KLF2 in various fibrotic diseases [27,28]. To the best of our knowledge, this is the first study that attempts to shed light on the role of KLF2 in LFs at COVID-19 environment and correlate its expression with the immunofibrotic aspect of these cells. KLF2 was inversely correlated with CCN2 in LFs, at mRNA, protein and functional wound healing assay level. Interestingly, COMBI-treated fibroblasts, restored their low KLF2 levels to normal and abolished their CCN2-related fibrotic potential. In addition, tannic acid, a plant-derived polyphenol acting as a natural inducer of KLF2 [36] was not able to restore the suppressed expression of KLF2 levels in LFs cultures triggered by COVID-19 inflammatory environment. Taken together, these findings support the involvement of multiple inflammatory signals in the expression of KLF2 in LFs during an aberrant immunofibrotic response in severe COVID-19. Indeed, recent data demonstrated an association of inflammatory responses and persistent NETosis with fibrotic processes and impaired lung function in patients that had been severely affected by SARS-CoV-2 [64,65].

Recently, we reported that COMBI therapeutic protocol has favorable effect in severe COVID-19 patients and may inhibit plasma-induced TF/thrombin pathway in primary LFs suggesting an important role for these cells in disease pathogenesis [17]. Trying to validate these findings and further investigate the mechanistic basis behind the immunofibrotic role of LFs, we analyzed the effect of COMBI treatment by almost doubling the number of patients. We found similar to the previously reported rates of intubation/ICU admission and in-hospital mortality, confirming the beneficial effect of combined rescue strategy in severe COVID-19.

In parallel, we investigated the fibrotic behavior of plasma from COVID-19 patients with severe respiratory failure under or not COMBI treatment. In correspondence to our clinical results, stimulation of LFs, with plasma derived from COMBI-treated patients, seven days after the initiation of treatment, was associated with reduction of CCN2 and increase of KLF2 levels, compared to the plasma collected at the day of admission. In contrast, plasma samples collected from SOC-only-treated patients, during the same timepoints as in COMBI protocol, did not induce significant alterations on CCN2 and KLF2 expression in cultured LFs. We suggest that the plasma obtained from COMBI-treated patients mitigates the pre-fibrotic behavior of LFs, while the simultaneous restoration of KLF2 levels highlights its involvement as a potent regulator of the immunofibrotic process. Although KLF2 expression seems to be linked with fibrotic potency, *via* a cross-talk between NETs, JAK, IL-6 signaling, further studies are needed to explore in detail the puzzle of immunofibrosis.

Interstitial lung diseases (ILDs) comprise a group of disorders associated with various etiologies such as infections, radiation, drugs and systemic autoimmune diseases. Similarly, to COVID-19 lung disease, ILDs are characterized by lung fibroblast activation, interstitial inflammation, and fibrotic lung damage [66]. Over the last years, multiple mechanism-based immunomodulatory therapies, including tocilizumab or JAK inhibitors, have been used as salvage treatment in refractory and progressive ILDs [60,67,68]. Of note, it has been proposed that immunomodulation might be effective particularly in early disease with higher levels of inflammatory activity [67]. The present study, despite the limitations of the non-randomized design and small number of patients, suggests that early combination of immunomodulatory agents targeting distinct inflammatory pathways could be a promising and safe therapeutic option in complex immune-mediated fibrotic diseases, such as COVID-19.

In conclusion, regulation of KLF2 expression in LFs appears as an important mechanism linking aberrant host inflammatory responses with fibrotic process in severe COVID-19. Rescue combination treatment, with inhaled DNase I and baricitinib plus tocilizumab, may be effective in patients with severe respiratory failure by targeting this mechanism. Further investigation of molecular pathways and mechanisms that govern KLF2 expression in LFs could provide novel diagnostic and/or therapeutic targets for severe cases of acute and post-acute SARS-CoV-2 infection, as well as for other immunofibrotic lung diseases.

Author contributions

AC methodology, investigation, writing - original draft; CA investigation, resources, writing - original draft; AMN investigation, visualization, writing - original draft; EG visualization, resources, writing - original draft; VP formal analysis, writing - review & editing; EX, SD investigation, validation, DM resources; VT investigation; KK, MK validation, writing - review & editing; PS, KR conceptualization, writing - review & editing, supervision, project administration, funding acquisition. All authors have read and approved the final manuscript.

Funding

This study was supported by the Greek General Secretariat for Research and Technology (GSRT), Research & Innovation Programme CytoNET, grant MIS-5048548 and by GSRT, Regional Excellence Programme InTechThrace, grant MIS-5047285.

Declaration of Competing Interest

The authors have declared that no conflict of interest exists.

Data availability

Data will be made available on request.

Acknowledgements

We would like to thank the BioImaging-Democritus University of Thrace (DUTH) facility.

Appendix A. Supplementary data

Supplementary data to this article can be found online at https://doi.org/10.1016/j.clim.2023.109240.

References

[1] P.M. George, A.U. Wells, R.G. Jenkins, Pulmonary fibrosis and COVID-19: the potential role for antifibrotic therapy, Lancet Respir. Med. 8 (2020) 807–815, https://doi.org/10.1016/S2213-2600(20)30225-3.

[2] B.J. Hama Amin, F.H. Kakamad, G.S. Ahmed, S.F. Ahmed, B.A. Abdulla, S. H. Mohammed, T.M. Mikael, R.Q. Salih, R.K. Ali, A.M. Salh, D.A. Hussein, Post COVID-19 pulmonary fibrosis; a meta-analysis study, Ann. Med. Surg. 2012 (77) (2022), 103590, https://doi.org/10.1016/j.amsu.2022.103590.

[3] A. Nalbandian, K. Sehgal, A. Gupta, M.V. Madhavan, C. McGroder, J.S. Stevens, J. R. Cook, A.S. Nordvig, D. Shalev, T.S. Sehrawat, N. Ahluwalia, B. Bikdeli, D. Dietz, C. Der-Nigoghossian, N. Liyanage-Don, G.F. Rosner, E.J. Bernstein, S. Mohan, A. A. Beckley, D.S. Seres, T.K. Choueiri, N. Uriel, J.C. Ausiello, D. Accili, D. E. Freedberg, M. Baldwin, A. Schwartz, D. Brodie, C.K. Garcia, M.S.V. Elkind, J. M. Connors, J.P. Bilezikian, D.W. Landry, E.Y. Wan, Post-acute COVID-19 syndrome, Nat. Med. 27 (2021) 601–615, https://doi.org/10.1038/s41591-021-01283-z.

[4] J.C. Melms, J. Biermann, H. Huang, Y. Wang, A. Nair, S. Tagore, I. Katsyv, A. F. Rendeiro, A.D. Amin, D. Schapiro, C.J. Frangieh, A.M. Luoma, A. Filliol, Y. Fang,

H. Ravichandran, M.G. Clausi, G.A. Alba, M. Rogava, S.W. Chen, P. Ho, D. T. Montoro, A.E. Kornberg, A.S. Han, M.F. Bakhoum, N. Anandasabapathy, M. Suárez-Fariñas, S.F. Bakhoum, Y. Bram, A. Borczuk, X.V. Guo, J.H. Lefkowitch, C. Marboe, S.M. Lagana, A. Del Portillo, E.J. Tsai, E. Zorn, G.S. Markowitz, R. F. Schwabe, R.E. Schwartz, O. Elemento, A. Saqi, H. Hibshoosh, J. Que, B. Izar, A molecular single-cell lung atlas of lethal COVID-19, Nature. 595 (2021) 114–119, https://doi.org/10.1038/s41586-021-03569-1.

[5] C. Huang, L. Huang, Y. Wang, X. Li, L. Ren, X. Gu, L. Kang, L. Guo, M. Liu, X. Zhou, J. Luo, Z. Huang, S. Tu, Y. Zhao, L. Chen, D. Xu, Y. Li, C. Li, L. Peng, Y. Li, W. Xie, D. Cui, L. Shang, G. Fan, J. Xu, G. Wang, Y. Wang, J. Zhong, C. Wang, J. Wang, D. Zhang, B. Cao, 6-month consequences of COVID-19 in patients discharged from hospital: a cohort study, Lancet Lond. Engl. 397 (2021) 220–232, https://doi.org/10.1016/S0140-6736(20)32656-8.

[6] S.B. Polak, I.C. Van Gool, D. Cohen, J.H. von der Thüsen, J. van Paassen, A systematic review of pathological findings in COVID-19: a pathophysiological timeline and possible mechanisms of disease progression, Mod. Pathol. Off. J. U. S. Can. Acad. Pathol. Inc. 33 (2020) 2128–2138, https://doi.org/10.1038/s41379-020-0603-3.

[7] E. Bazdyrev, P. Rusina, M. Panova, F. Novikov, I. Grishagin, V. Nebolsin, Lung fibrosis after COVID-19: treatment prospects, Pharm. Basel Switz. 14 (2021) 807, https://doi.org/10.3390/ph14080807.

[8] D. Wendisch, O. Dietrich, T. Mari, S. von Stillfried, I.L. Ibarra, M. Mittermaier, C. Mache, R.L. Chua, R. Knoll, S. Timm, S. Brumhard, T. Krammer, H. Zauber, A. L. Hiller, A. Pascual-Reguant, R. Mothes, R.D. Bülow, J. Schulze, A.M. Leipold, S. Djudjaj, F. Erhard, R. Geffers, F. Pott, J. Kazmierski, J. Radke, P. Pergantis, K. Baßler, C. Conrad, A.C. Aschenbrenner, B. Sawitzki, M. Landthaler, E. Wyler, D. Horst, S. Hippenstiel, A. Hocke, F.L. Heppner, A. Uhrig, C. Garcia, F. Machleidt, S. Herold, S. Elezkurtaj, C. Thibeault, M. Witzenrath, C. Cochain, N. Suttorp, C. Drosten, C. Goffinet, F. Kurth, J.L. Schultze, H. Radbruch, M. Ochs, R. Eils, H. Müller-Redetzky, A.E. Hauser, M.D. Luecken, F.J. Theis, C. Conrad, T. Wolff, P. Boor, M. Selbach, A.-E. Saliba, L.E. Sander, SARS-CoV-2 infection triggers profibrotic macrophage responses and lung fibrosis, Cell. 184 (2021) 6243–6261. e27, https://doi.org/10.1016/j.cell.2021.11.033.

[9] M. Kiener, N. Roldan, C. Machahua, A. Sengupta, T. Geiser, O.T. Guenat, M. Funke-Chambour, N. Hobi, M. Kruithof-de Julio, Human-based advanced in vitro approaches to investigate lung fibrosis and pulmonary effects of COVID-19, Front. Med. 8 (2021), 644678, https://doi.org/10.3389/fmed.2021.644678.

[10] A.F. Rendeiro, H. Ravichandran, Y. Bram, V. Chandar, J. Kim, C. Meydan, J. Park, J. Foox, T. Hether, S. Warren, Y. Kim, J. Reeves, S. Salvatore, C.E. Mason, E. C. Swanson, A.C. Borczuk, O. Elemento, R.E. Schwartz, The spatial landscape of lung pathology during COVID-19 progression, Nature. 593 (2021) 564–569, https://doi.org/10.1038/s41586-021-03475-6.

[11] S. Wang, X. Yao, S. Ma, Y. Ping, Y. Fan, S. Sun, Z. He, Y. Shi, L. Sun, S. Xiao, M. Song, J. Cai, J. Li, R. Tang, L. Zhao, C. Wang, Q. Wang, L. Zhao, H. Hu, X. Liu, G. Sun, L. Chen, G. Pan, H. Chen, Q. Li, P. Zhang, Y. Xu, H. Feng, G.-G. Zhao, T. Wen, Y. Yang, X. Huang, W. Li, Z. Liu, H. Wang, H. Wu, B. Hu, Y. Ren, Q. Zhou, J. Qu, W. Zhang, G.-H. Liu, X.-W. Bian, A single-cell transcriptomic landscape of the lungs of patients with COVID-19, Nat. Cell Biol. 23 (2021) 1314–1328, https://doi.org/10.1038/s41556-021-00796-6.

[12] A.E. John, C. Joseph, G. Jenkins, A.L. Tatler, COVID-19 and pulmonary fibrosis: A potential role for lung epithelial cells and fibroblasts, Immunol. Rev. 302 (2021) 228–240, https://doi.org/10.1111/imr.12977.

[13] P. Skendros, A. Mitsios, A. Chrysanthopoulou, D.C. Mastellos, S. Metallidis, P. Rafailidis, M. Ntinopoulou, E. Sertaridou, V. Tsironidou, C. Tsigalou, M. Tektonidou, T. Konstantinidis, C. Papagoras, I. Mitroulis, G. Germanidis, J. D. Lambris, K. Ritis, Complement and tissue factor–enriched neutrophil extracellular traps are key drivers in COVID-19 immunothrombosis, J. Clin. Invest. 130 (2020) 6151–6157, https://doi.org/10.1172/JCI141374.

[14] M. Ackermann, S.E. Verleden, M. Kuehnel, A. Haverich, T. Welte, F. Laenger, A. Vanstapel, C. Werlein, H. Stark, A. Tzankov, W.W. Li, V.W. Li, S.J. Mentzer, D. Jonigk, Pulmonary vascular Endothelialitis, thrombosis, and angiogenesis in Covid-19, N. Engl. J. Med. 383 (2020) 120–128, https://doi.org/10.1056/NEJMoa2015432.

[15] K.E. Lipson, C. Wong, Y. Teng, S. Spong, CTGF is a central mediator of tissue remodeling and fibrosis and its inhibition can reverse the process of fibrosis, Fibrogenesis Tissue Repair 5 (2012) S24, https://doi.org/10.1186/1755-1536-5-S1-S24.

[16] M. Ponticos, A.M. Holmes, X. Shi-Wen, P. Leoni, K. Khan, V.S. Rajkumar, R. K. Hoyles, G. Bou-Gharios, C.M. Black, C.P. Denton, D.J. Abraham, A. Leask, G. E. Lindahl, Pivotal role of connective tissue growth factor in lung fibrosis: MAPK-dependent transcriptional activation of type I collagen, Arthritis Rheum. 60 (2009) 2142–2155, https://doi.org/10.1002/art.24620.

[17] E. Gavriilidis, C. Antoniadou, A. Chrysanthopoulou, M. Ntinopoulou, A. Smyrlis, I. Fotiadou, N. Zioga, D. Kogias, A.-M. Natsi, C. Pelekoudas, E. Satiridou, S.-A. Bakola, C. Papagoras, I. Mitroulis, P. Peichamperis, D. Mikroulis, V. Papadopoulos, P. Skendros, K. Ritis, Combined administration of inhaled DNase, baricitinib and tocilizumab as rescue treatment in COVID-19 patients with severe respiratory failure, Clin. Immunol. 238 (2022), 109016, https://doi.org/10.1016/j.clim.2022.109016.

[18] R.T. Kendall, C.A. Feghali-Bostwick, Fibroblasts in fibrosis: novel roles and mediators, Front. Pharmacol. 5 (2014) 123, https://doi.org/10.3389/fphar.2014.00123.

[19] M.V. Plikus, X. Wang, S. Sinha, E. Forte, S.M. Thompson, E.L. Herzog, R.R. Driskell, N. Rosenthal, J. Biernaskie, V. Horsley, Fibroblasts: origins, definitions, and functions in health and disease, Cell. 184 (2021) 3852–3872, https://doi.org/10.1016/j.cell.2021.06.024.

[20] K.T. Turpaev, Transcription factor KLF2 and its role in the regulation of inflammatory processes, Biochem. Mosc. 85 (2020) 54–67, https://doi.org/10.1134/S0006297920010058.

[21] L. Nayak, L. Goduni, Y. Takami, N. Sharma, P. Kapil, M.K. Jain, G. H. Mahabeleshwar, Kruppel-like factor 2 is a transcriptional regulator of chronic and acute inflammation, Am. J. Pathol. 182 (2013) 1696–1704, https://doi.org/10.1016/j.ajpath.2013.01.029.

[22] X. Tang, P. Wang, R. Zhang, I. Watanabe, E. Chang, V. Vinayachandran, L. Nayak, S. Lapping, S. Liao, A. Madera, D.R. Sweet, J. Luo, J. Fei, H.-W. Jeong, R.H. Adams, T. Zhang, X. Liao, M.K. Jain, KLF2 regulates neutrophil activation and thrombosis in cardiac hypertrophy and heart failure progression, J. Clin. Invest. 132 (2022), e147191, https://doi.org/10.1172/JCI147191.

[23] Z. Varga, A.J. Flammer, P. Steiger, M. Haberecker, R. Andermatt, A.S. Zinkernagel, M.R. Mehra, R.A. Schuepbach, F. Ruschitzka, H. Moch, Endothelial cell infection and endotheliitis in COVID-19, Lancet Lond. Engl. 395 (2020) 1417–1418, https://doi.org/10.1016/S0140-6736(20)30937-5.

[24] D. Wu, T.-H. Lee, R.-T. Huang, R.D. Guzy, N. Schoettler, A. Adegunsoye, J. Mueller, A. Husain, A.I. Sperling, G.M. Mutlu, Y. Fang, SARS-CoV-2 infection is associated with reduced Krüppel-like factor 2 in human lung autopsy, Am. J. Respir. Cell Mol. Biol. 65 (2021) 222–226, https://doi.org/10.1165/rcmb.2020-0564LE.

[25] R.-T. Huang, D. Wu, A. Meliton, M.-J. Oh, M. Krause, J.A. Lloyd, R. Nigdelioglu, R. B. Hamanaka, M.K. Jain, A. Birukova, J.P. Kress, K.G. Birukov, G.M. Mutlu, Y. Fang, Experimental lung injury reduces Krüppel-like factor 2 to increase endothelial permeability via regulation of RAPGEF3-Rac1 signaling, Am. J. Respir. Crit. Care Med. 195 (2017) 639–651, https://doi.org/10.1164/rccm.201604-0668OC.

[26] S. Xu, Y. Liu, Y. Ding, S. Luo, X. Zheng, X. Wu, Z. Liu, I. Ilyas, S. Chen, S. Han, P. J. Little, M.K. Jain, J. Weng, The zinc finger transcription factor, KLF2, protects against COVID-19 associated endothelial dysfunction, Sign. Transduct. Target. Ther. 6 (2021) 266, https://doi.org/10.1038/s41392-021-00690-5.

[27] J. Shi, L. Zhou, X. Wang, J. Du, M. Jiang, Z. Song, G. Han, Z. Mai, KLF2 attenuates bleomycin-induced pulmonary fibrosis and inflammation with regulation of AP-1, Biochem. Biophys. Res. Commun. 495 (2018) 20–26, https://doi.org/10.1016/j.bbrc.2017.10.114.

[28] G. Marrone, R. Maeso-Díaz, G. García-Cardena, J.G. Abraldes, J.C. García-Pagán, J. Bosch, J. Gracia-Sancho, KLF2 exerts antifibrotic and vasoprotective effects in cirrhotic rat livers: behind the molecular mechanisms of statins, Gut. 64 (2015) 1434–1443, https://doi.org/10.1136/gutjnl-2014-308338.

[29] G. Linklater, S. Lawton, S. Fielding, L. Macaulay, D. Carroll, D. Pang, Introducing the palliative performance scale to clinicians: the Grampian experience, BMJ Support. Palliat. Care 2 (2012) 121–126, https://doi.org/10.1136/bmjspcare-2011-000133.

[30] A. Ferrante, Y.H. Thong, Optimal conditions for simultaneous purification of mononuclear and polymorphonuclear leucocytes from human blood by the hypaque-ficoll method, J. Immunol. Methods 36 (1980) 109–117, https://doi.org/10.1016/0022-1759(80)90036-8.

[31] D.A. Stakos, K. Kambas, T. Konstantinidis, I. Mitroulis, E. Apostolidou, S. Arelaki, V. Tsironidou, A. Giatromanolaki, P. Skendros, S. Konstantinides, K. Ritis, Expression of functional tissue factor by neutrophil extracellular traps in culprit artery of acute myocardial infarction, Eur. Heart J. 36 (2015) 1405–1414, https://doi.org/10.1093/eurheartj/ehv007.

[32] M. Saffarzadeh, C. Juenemann, M.A. Queisser, G. Lochnit, G. Barreto, S.P. Galuska, J. Lohmeyer, K.T. Preissner, Neutrophil extracellular traps directly induce epithelial and endothelial cell death: a predominant role of histones, PLoS One 7 (2012), e32366, https://doi.org/10.1371/journal.pone.0032366.

[33] A. Caudrillier, K. Kessenbrock, B.M. Gilliss, J.X. Nguyen, M.B. Marques, M. Monestier, P. Toy, Z. Werb, M.R. Looney, Platelets induce neutrophil extracellular traps in transfusion-related acute lung injury, J. Clin. Invest. 122 (2012) 2661–2671, https://doi.org/10.1172/JCI61303.

[34] A. Chrysanthopoulou, I. Mitroulis, E. Apostolidou, S. Arelaki, D. Mikroulis, T. Konstantinidis, E. Sivridis, M. Koffa, A. Giatromanolaki, D.T. Boumpas, K. Ritis, K. Kambas, Neutrophil extracellular traps promote differentiation and function of fibroblasts, J. Pathol. 233 (2014) 294–307, https://doi.org/10.1002/path.4359.

[35] A. Chrysanthopoulou, I. Mitroulis, K. Kambas, P. Skendros, I. Kourtzelis, S. Vradelis, G. Kolios, S. Aslanidis, M. Doumas, K. Ritis, Tissue factor-thrombin signaling enhances the fibrotic activity of myofibroblasts in systemic sclerosis through up-regulation of endothelin receptor A, Arthritis Rheum. 63 (2011) 3586–3597, https://doi.org/10.1002/art.30586.

[36] Y. Xu, P. Liu, S. Xu, M. Koroleva, S. Zhang, S. Si, Z.G. Jin, Tannic acid as a plant-derived polyphenol exerts vasoprotection via enhancing KLF2 expression in endothelial cells, Sci. Rep. 7 (2017) 6686, https://doi.org/10.1038/s41598-017-06803-x.

[37] K.J. Livak, T.D. Schmittgen, Analysis of relative gene expression data using real-time quantitative PCR and the $2^{-\Delta\Delta CT}$ method, Methods. 25 (2001) 402–408, https://doi.org/10.1006/meth.2001.1262.

[38] A. Chrysanthopoulou, E. Gkaliagkousi, A. Lazaridis, S. Arelaki, P. Pateinakis, M. Ntinopoulou, A. Mitsios, C. Antoniadou, C. Argyriou, G.S. Georgiadis, V. Papadopoulos, A. Giatromanolaki, K. Ritis, P. Skendros, Angiotensin II triggers release of neutrophil extracellular traps, linking thromboinflammation with essential hypertension, JCI Insight. 6 (2021) e148668, https://doi.org/10.1172/jci.insight.148668.

[39] V. Knight, J. Tchongue, D. Lourensz, P. Tipping, W. Sievert, Protease-activated receptor 2 promotes experimental liver fibrosis in mice and activates human hepatic stellate cells, Hepatol. Baltim. Md. 55 (2012) 879–887, https://doi.org/10.1002/hep.24784.

[40] J.N. Gustine, D. Jones, Immunopathology of Hyperinflammation in COVID-19, Am. J. Pathol. 191 (2021) 4–17, https://doi.org/10.1016/j.ajpath.2020.08.009.
[41] T.M. Delorey, C.G.K. Ziegler, G. Heimberg, R. Normand, Y. Yang, Å. Segerstolpe, D. Abbondanza, S.J. Fleming, A. Subramanian, D.T. Montoro, K.A. Jagadeesh, K. K. Dey, P. Sen, M. Slyper, Y.H. Pita-Juárez, D. Phillips, J. Biermann, Z. Bloom-Ackermann, N. Barkas, A. Ganna, J. Gomez, J.C. Melms, I. Katsyv, E. Normandin, P. Naderi, Y.V. Popov, S.S. Raju, S. Niezen, L.T.-Y. Tsai, K.J. Siddle, M. Sud, V. M. Tran, S.K. Vellarikkal, Y. Wang, L. Amir-Zilberstein, D.S. Atri, J. Beechem, O. R. Brook, J. Chen, P. Divakar, P. Dorceus, J.M. Engreitz, A. Essene, D.M. Fitzgerald, R. Fropf, S. Gazal, J. Gould, J. Grzyb, T. Harvey, J. Hecht, T. Hether, J. Jané-Valbuena, M. Leney-Greene, H. Ma, C. McCabe, D.E. McLoughlin, E.M. Miller, C. Muus, M. Niemi, R. Padera, L. Pan, D. Pant, C. Pe'er, J. Pfiffner-Borges, C. J. Pinto, J. Plaisted, J. Reeves, M. Ross, M. Rudy, E.H. Rueckert, M. Siciliano, A. Sturm, E. Todres, A. Waghray, S. Warren, S. Zhang, D.R. Zollinger, L. Cosimi, R. M. Gupta, N. Hacohen, H. Hibshoosh, W. Hide, A.L. Price, J. Rajagopal, P.R. Tata, S. Riedel, G. Szabo, T.L. Tickle, P.T. Ellinor, D. Hung, P.C. Sabeti, R. Novak, R. Rogers, D.E. Ingber, Z.G. Jiang, D. Juric, M. Babadi, S.L. Farhi, B. Izar, J. R. Stone, I.S. Vlachos, I.H. Solomon, O. Ashenberg, C.B.M. Porter, B. Li, A. K. Shalek, A.-C. Villani, O. Rozenblatt-Rosen, A. Regev, COVID-19 tissue atlases reveal SARS-CoV-2 pathology and cellular targets, Nature 595 (2021) 107–113, https://doi.org/10.1038/s41586-021-03570-8.
[42] A. Santa Cruz, A. Mendes-Frias, A.I. Oliveira, L. Dias, A.R. Matos, A. Carvalho, C. Capela, J. Pedrosa, A.G. Castro, R. Silvestre, Interleukin-6 is a biomarker for the development of fatal severe acute respiratory syndrome coronavirus 2 pneumonia, Front. Immunol. 12 (2021), 613422, https://doi.org/10.3389/fimmu.2021.613422.
[43] T. Tanaka, M. Narazaki, T. Kishimoto, IL-6 in inflammation, immunity, and disease, Cold Spring Harb. Perspect. Biol. 6 (2014) a016295, https://doi.org/10.1101/cshperspect.a016295.
[44] C. Salama, J. Han, L. Yau, W.G. Reiss, B. Kramer, J.D. Neidhart, G.J. Criner, E. Kaplan-Lewis, R. Baden, L. Pandit, M.L. Cameron, J. Garcia-Diaz, V. Chávez, M. Mekebeb-Reuter, F. Lima de Menezes, R. Shah, M.F. González-Lara, B. Assman, J. Freedman, S.V. Mohan, Tocilizumab in patients hospitalized with Covid-19 pneumonia, N. Engl. J. Med. 384 (2021) 20–30, https://doi.org/10.1056/NEJMoa2030340.
[45] J.M. Connors, J.H. Levy, COVID-19 and its implications for thrombosis and anticoagulation, Blood. 135 (2020) 2033–2040, https://doi.org/10.1182/blood.2020006000.
[46] V.C. Marconi, A.V. Ramanan, S. de Bono, C.E. Kartman, V. Krishnan, R. Liao, M.L. B. Piruzeli, J.D. Goldman, J. Alatorre-Alexander, R. de Cassia Pellegrini, V. Estrada, M. Som, A. Cardoso, S. Chakladar, B. Crowe, P. Reis, X. Zhang, D.H. Adams, E. W. Ely, M.-Y. Ahn, M. Akasbi, J. Alatorre-Alexander, J.D. Altclas, F. Ariel, H. A. Ariza, C. Atkar, A. Bertetti, M. Bhattacharya, M.L. Briones, A. Budhraja, A. Burza, A. Camacho Ortiz, R. Caricchio, M. Casas, V. Cevoli Recio, W.S. Choi, E. Cohen, A. Comulada-Rivera, P. Cook, D.P. Cornejo Juarez, C. Daniel, L.F. Degrecci Relvas, J.G. Dominguez Cherit, T. Ellerin, D. Enikeev, S. Erico Tanni Minamoto, V. Estrada, E. Fiss, M. Furuichi, K. Giovanni Luz, J.D. Goldman, O. Gonzalez, I. Gordeev, T. Gruenewald, V.A. Hamamoto Sato, E.Y. Heo, J.Y. Heo, M. Hermida, Y. Hirai, D. Hutchinson, C. Iastrebner, O. Ioachimescu, M. Jain, M.P. Juliani Souza Lima, A. Khan, A.E. Kremer, T. Lawrie, M. MacElwee, F. Madhani-Lovely, V. Malhotra, M.F. Martínez Resendez, J. McKinnell, P. Milligan, C. Minelli, M.A. Moran Rodriguez, M.L. Parody, P. Paulin, R.C. de Pellegrini, P. Pemu, A.C. Procopio Carvalho, M. Puoti, J. Purow, M. Ramesh, A. Rea Neto, A. Rea Neto, P. Robinson, C. Rodrigues, G. Rojas Velasco, J.F.K. Saraiva, M. Scheinberg, S. Schreiber, D. Scublinsky, A. Sevciovic Grumach, I. Shawa, J. Simon Campos, N. Sofat, M. Som, C.D. Spinner, E. Sprinz, R. Stienecker, J. Suarez, N. Tachikawa, H. Tahir, B. Tiffany, A. Vishnevsky, A. Westheimer Cavalcante, K. Zirpe, Efficacy and safety of baricitinib for the treatment of hospitalised adults with COVID-19 (COV-BARRIER): a randomised, double-blind, parallel-group, placebo-controlled phase 3 trial, Lancet Respir. Med. 9 (2021) 1407–1418, https://doi.org/10.1016/S2213-2600(21)00331-3.
[47] Z.M. Holliday, A.P. Earhart, M.M. Alnijoumi, A. Krvavac, L.-A.H. Allen, A. G. Schrum, Non-randomized trial of Dornase alfa for acute respiratory distress syndrome secondary to Covid-19, Front. Immunol. 12 (2021), 714833, https://doi.org/10.3389/fimmu.2021.714833.
[48] A. Toma, C. Darwish, M. Taylor, J. Harlacher, R. Darwish, The use of Dornase alfa in the management of COVID-19-associated adult respiratory distress syndrome, Crit. Care Res. Pract. 2021 (2021) 1–6, https://doi.org/10.1155/2021/8881115.
[49] C. Magro, J.J. Mulvey, D. Berlin, G. Nuovo, S. Salvatore, J. Harp, A. Baxter-Stoltzfus, J. Laurence, Complement associated microvascular injury and thrombosis in the pathogenesis of severe COVID-19 infection: A report of five cases, Transl. Res. 220 (2020) 1–13, https://doi.org/10.1016/j.trsl.2020.04.007.
[50] A. Bonaventura, A. Vecchié, L. Dagna, K. Martinod, D.L. Dixon, B.W. Van Tassell, F. Dentali, F. Montecucco, S. Massberg, M. Levi, A. Abbate, Endothelial dysfunction and immunothrombosis as key pathogenic mechanisms in COVID-19, Nat. Rev. Immunol. 21 (2021) 319–329, https://doi.org/10.1038/s41577-021-00536-9.
[51] D.A. Berlin, R.M. Gulick, F.J. Martinez, Severe Covid-19, N. Engl. J. Med. 383 (2020) 2451–2460, https://doi.org/10.1056/NEJMcp2009575.
[52] K. Martinod, T. Witsch, L. Erpenbeck, A. Savchenko, H. Hayashi, D. Cherpokova, M. Gallant, M. Mauler, S.M. Cifuni, D.D. Wagner, Peptidylarginine deiminase 4 promotes age-related organ fibrosis, J. Exp. Med. 214 (2017) 439–458, https://doi.org/10.1084/jem.20160530.
[53] E. Frangou, A. Chrysanthopoulou, A. Mitsios, K. Kambas, S. Arelaki, I. Angelidou, A. Arampatzioglou, H. Gakiopoulou, G.K. Bertsias, P. Verginis, K. Ritis, D. T. Boumpas, REDD1/autophagy pathway promotes thromboinflammation and fibrosis in human systemic lupus erythematosus (SLE) through NETs decorated with tissue factor (TF) and interleukin-17A (IL-17A), Ann. Rheum. Dis. 78 (2019) 238–248, https://doi.org/10.1136/annrheumdis-2018-213181.
[54] K. Didier, D. Giusti, S. Le Jan, C. Terryn, C. Muller, B.N. Pham, R. Le Naour, F. D. Antonicelli, A. Servettaz, Neutrophil extracellular traps generation relates with early stage and vascular complications in systemic sclerosis, J. Clin. Med. 9 (2020) E2136, https://doi.org/10.3390/jcm9072136.
[55] M. Negreros, L.F. Flores-Suárez, A proposed role of neutrophil extracellular traps and their interplay with fibroblasts in ANCA-associated vasculitis lung fibrosis, Autoimmun. Rev. 20 (2021), 102781, https://doi.org/10.1016/j.autrev.2021.102781.
[56] Y. Wang, Y. Li, Z. Chen, Y. Yuan, Q. Su, K. Ye, C. Chen, G. Li, Y. Song, H. Chen, Y. Xu, GSDMD-dependent neutrophil extracellular traps promote macrophage-to-myofibroblast transition and renal fibrosis in obstructive nephropathy, Cell Death Dis. 13 (2022) 693, https://doi.org/10.1038/s41419-022-05138-4.
[57] M. Wygrecka, D. Zakrzewicz, B. Taborski, M. Didiasova, G. Kwapiszewska, K. T. Preissner, P. Markart, TGF-β1 induces tissue factor expression in human lung fibroblasts in a PI3K/JNK/Akt-dependent and AP-1-dependent manner, Am. J. Respir. Cell Mol. Biol. 47 (2012) 614–627, https://doi.org/10.1165/rcmb.2012-0097OC.
[58] S. Torres, C. Ortiz, N. Bachtler, W. Gu, L.D. Grünewald, N. Kraus, R. Schierwagen, C. Hieber, C. Meier, O. Tyc, M. Joseph Brol, F.E. Uschner, B. Nijmeijer, C. Welsch, M.-L. Berres, C. Garcia-Ruiz, J.C. Fernandez-Checa, C. Trautwein, T.J. Vogl, S. Zeuzem, J. Trebicka, S. Klein, Janus kinase 2 inhibition by pacritinib as potential therapeutic target for liver fibrosis, Hepatol. Baltim. Md. (2022), https://doi.org/10.1002/hep.32746.
[59] C. Moriana, T. Moulinet, R. Jaussaud, P. Decker, JAK inhibitors and systemic sclerosis: A systematic review of the literature, Autoimmun. Rev. 21 (2022), 103168, https://doi.org/10.1016/j.autrev.2022.103168.
[60] R. Huo, Q. Guo, J. Hu, N. Li, R. Gao, L. Mi, Z. Zhang, H. Liu, Z. Guo, H. Zhao, L. Zhang, K. Xu, Therapeutic potential of Janus kinase inhibitors for the management of interstitial lung disease, Drug Des. Devel. Ther. 16 (2022) 991–998, https://doi.org/10.2147/DDDT.S353494.
[61] Y. Tanaka, Y. Luo, J.J. O'Shea, S. Nakayamada, Janus kinase-targeting therapies in rheumatology: a mechanisms-based approach, Nat. Rev. Rheumatol. 18 (2022) 133–145, https://doi.org/10.1038/s41584-021-00726-8.
[62] M. d'Alessandro, F. Perillo, R. Metella Refini, L. Bergantini, F. Bellisai, E. Selvi, P. Cameli, S. Manganelli, E. Conticini, L. Cantarini, P. Sestini, B. Frediani, E. Bargagli, Efficacy of baricitinib in treating rheumatoid arthritis: modulatory effects on fibrotic and inflammatory biomarkers in a real-life setting, Int. Immunopharmacol. 86 (2020), 106748, https://doi.org/10.1016/j.intimp.2020.106748.
[63] L. Nayak, D.R. Sweet, A. Thomas, S.D. Lapping, K. Kalikasingh, A. Madera, V. Vinayachandran, R. Padmanabhan, N.T. Vasudevan, J.T. Myers, A.Y. Huang, A. Schmaier, N. Mackman, X. Liao, A. Maiseyeu, M.K. Jain, A targetable pathway in neutrophils mitigates both arterial and venous thrombosis, Sci. Transl. Med. 14 (2022) eabj7465, https://doi.org/10.1126/scitranslmed.abj7465.
[64] H.J. Chun, E. Coutavas, A.B. Pine, A.I. Lee, V.L. Yu, M.K. Shallow, C. X. Giovacchini, A.M. Mathews, B. Stephenson, L.G. Que, P.J. Lee, B.D. Kraft, Immunofibrotic drivers of impaired lung function in postacute sequelae of SARS-CoV-2 infection, JCI Insight. 6 (2021), 148476, https://doi.org/10.1172/jci.insight.148476.
[65] P.M. George, A. Reed, S.R. Desai, A. Devaraj, T.S. Faiez, S. Laverty, A. Kanwal, C. Esneau, M.K.C. Liu, F. Kamal, W.D.-C. Man, S. Kaul, S. Singh, G. Lamb, F. K. Faizi, M. Schuliga, J. Read, T. Burgoyne, A.L. Pinto, J. Micallef, E. Bauwens, J. Candiracci, M. Bougoussa, M. Herzog, L. Raman, B. Ahmetaj-Shala, S. Turville, A. Aggarwal, H.A. Farne, A. Dalla Pria, A.D. Aswani, F. Patella, W.E. Borek, J. A. Mitchell, N.W. Bartlett, A. Dokal, X.-N. Xu, P. Kelleher, A. Shah, A. Singanayagam, A persistent neutrophil-associated immune signature characterizes post–COVID-19 pulmonary sequelae, Sci. Transl. Med. 14 (2022) eabo5795, https://doi.org/10.1126/scitranslmed.abo5795.
[66] T. Shao, X. Shi, S. Yang, W. Zhang, X. Li, J. Shu, S. Alqalyoobi, A.A. Zeki, P. S. Leung, Z. Shuai, Interstitial lung disease in connective tissue disease: a common lesion with heterogeneous mechanisms and treatment considerations, Front. Immunol. 12 (2021), 684699, https://doi.org/10.3389/fimmu.2021.684699.
[67] B. Seeliger, A. Prasse, Immunomodulation in autoimmune interstitial lung disease, Respir. Int. Rev. Thorac. Dis. 99 (2020) 819–829, https://doi.org/10.1159/000511200.
[68] F.V. Karakontaki, E.S. Panselinas, V.S. Polychronopoulos, A.G. Tzioufas, Targeted therapies in interstitial lung disease secondary to systemic autoimmune rheumatic disease. Current status and future development, Autoimmun. Rev. 20 (2021), 102742, https://doi.org/10.1016/j.autrev.2020.102742.